

# Selective Pulse Coupling Synchronicity for Sensor Network

Yu Niu, Brian J. d'Auriol, Xiaoling Wu, Jin Wang, Jinsung Cho, Sungyoung Lee \*  
Dept. of Computer Engineering, Kyung Hee University, Korea  
{niu, dauriol, xiaoling, wangjin, sylee}@oslab.khu.ac.kr  
chojs@khu.ac.kr

## Abstract

*Simple, fast, low energy consumption time synchronization protocol is needed by sensor networks. Mutual interaction synchronization is highly attractive for wireless sensor network for its simplicity, self-organization and good scalability. The proposed Selective Coupling Synchronicity Algorithm (SCSA) addresses the problem of low efficiency caused by the phase swing actions in the original all Pulse Coupling model. The benefits are fast synchronizing speed and associated low energy consumption. The simulation results show that our algorithm performs better than the original model in most situations.*

## 1. Introduction

Time synchronization is a critical piece of infrastructure in distributed systems and wireless sensor networks make particularly extensive use of synchronized time. Applications such as target tracking, MAC layer access schedule, or time varying data collection, need either local or global synchronized time scale as a precondition.

For the critical requirement and constraints of sensor networks, researchers proposed many time synchronization protocols. Centralized synchronization protocols (TPSN [2], FTSP [5], RBS [1]) are simple and can obtain reasonable precision, but the scalability and robustness usually is poor. Part distributed protocols ([8], RITS [4]) scale much better than centralized protocols in space and density, however usually the computing complexity is relatively high. The mutual interacting model inspired from biological self-synchronizing phenomena is completely different from these. It regards distributed agents as oscillators whose phases couple with each other when they 'hear' the pulse signal. It is simple, self-organizing, scalable, robust and has a long lifetime. All these salient features are suitable for sensor networks which are constructed by a large amount of small size, low computation ability, limited energy supplied sensor nodes.

The speed of synchronization is called the immediacy of the time synchronization protocol. To control this, the high level system parameters such as coupling strength [7] and oscillator density [3] are concerned in previous works. Different from these, based on our own Converging Direction Determinant Formula, the proposed Selective Coupling Synchronicity Algorithm modifies the intrinsic behavior of nodes. It predicts the upcoming reactions' converging direction and ignores some incoming pulses that may cause reverse direction actions so as to eliminates the blindness of oscillators' interaction and the unnecessary attempting works. Under the same condition, our algorithm can increase the converging speed, and save the associated energy consumption compared to the original pulse coupling model.

Our work has three main contributions: 1) the discussion in [7] is extended and enhanced to more clearly describe the dynamic nature of the converging process, in particular we derive the Converging Direction Determinant Formula; 2) besides inheriting the advantages of the pulse coupling model(simplicity, self-organization, robustness), our selective coupling synchronicity algorithm quicken the synchronizing speed under different parameter settings, and this can greatly reduce the network topology deployment requirement to guarantee the convergence in multi-hop situation; 3) while increasing the synchronizing speed, our algorithm also can save on the energy consumption for reducing the total message transmission amount.

The remainder of the paper is organized as follows. Section II introduces the pulse coupling model related work with a discussion on synchronization rate. Section III introduces the pulse coupling mathematical model and presents our own node Converging Direction Determinant Formula. Section IV presents the Selective Coupling Synchronicity Algorithm. Section V describes the algorithm performance evaluation and associated analysis. Section VI gives out the conclusion.

## 2 Related Work

The *synchronicity* is defined as the ability to organize simultaneous collective action across the whole network.

---

\*Prof. Sungyoung Lee is the corresponding author.

In [7] the biological individuals are regarded as the Pulse-Coupled biological Oscillators (PCO) and they proved that a very simple reactive node behavior would always converge to produce global synchronicity, regardless of the number of nodes and starting times. Later in [6], they lift the all-to-all communication requirement implicit in [7], so that the model can converge to a synchronized state based on the local communication topology only.

Many papers also give out discussion on the pulse coupling model synchronizing rate. The work in [7] models the oscillating function as  $(f(\phi) = \frac{1}{b} \ln(1 + [e^b - 1]\phi))$ . They mathematically prove that the time taken to synchronize is inversely proportional to the product  $\epsilon b$ , in which  $b$  measures the extent to which  $f$  is concave down and  $\epsilon$  is the coupling strength. Usually the sensor node's oscillating function is set fixed,  $b$  does not change frequently, we only adjust the coupling strength  $\epsilon$ . However,  $\epsilon$  can not be chosen arbitrarily large, the node may "overshoot" and prevent converging [11]. In [3] observations are made that, when the node density meets some threshold that makes  $\epsilon N(1 - p_{MD}) \geq 1$ , (where  $N$  is the node number in one broadcast range,  $p_{MD}$  is the probability of missed detections), the *avalanche effect* occurs with high probability. *Avalanche effect* means that the firing of one oscillator brings another to the firing threshold, the latter oscillator fires immediately and ignites a "chain reaction" of additional firing and locks the network into synchrony immediately. This effect requires that the oscillators can successively jump and fire or the pulse strength of a synchronous group is assumed to be the sum of the individual pulse strengths. However, for the existence of the oscillating refractory period, usually the latter oscillator is not allowed to fire until the next time it reaches the threshold. Also oscillators do not detect the pulse strength exactly for simplicity. This leads to choose the coupling parameter  $\epsilon$  under the constraints of hardware and network environment.

### 3 Converging direction determinant formula

#### 3.1 Pulse-Coupling Model

Today's computing devices are equipped with a hardware oscillator assisted clock. The pulse coupling model regards every distributed clock as an oscillator with the same fixed frequency but different initial phase. The coupling aim to eliminate the phase difference (to make them shrink to 0 or enlarge to 1) and let these oscillators act with the same phase and the same frequency, so-called getting synchronized. Oscillator phase  $\phi$  and state  $\varphi = f(\phi)$  both are defined on  $[0, 1]$ .  $f(\phi)$  is the oscillating function and should be monotonically increasing and concave down (that is:  $f' > 0$  and  $f'' < 0$ ;  $f(0) = 0$ ,  $f(1) = 1$ ). When there is only one oscillator, the state will follow the function curve from 0 to 1 at a regular rate:  $d\phi/dt = 1/T$  ( $T$  is the func-

tion cycle period). When the phase arrives at 1, it fires and emits a pulse, then resets the phase to 0 and starts a new cycle again. However, if during the walking path, at time  $t$ , it receives a pulse from the other oscillator, the state will jump an amount  $\epsilon$  and the phase be updated as (Figure 1):

$$\phi_{t'} = \begin{cases} f^{-1}(f(\phi_t) + \epsilon), & \text{if } f^{-1}(f(\phi_t) + \epsilon) < 1 \\ 0, & \text{otherwise} \end{cases}$$

Thus, all oscillators follow the same update equation when detect the firing pulse, they interact with each other and adjust their phases to an agreed one.

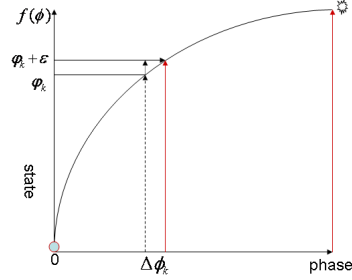


Figure 1. Oscillator jump action.

#### 3.2 Converging Direction Determinant Formula

To make sure the oscillators' phase difference converging direction, we draw a pair of nodes converging procedure in a single cycle (Figure 2). Since PCO is a discrete model and is controlled by few parameters, all the computations are pertinent to phases. Let vector  $|\overrightarrow{AB}|$ , the bold lines in Figure 2, represent the phase distance from  $A$  to  $B$ . Whenever  $|\overrightarrow{AB}|$  shrinks to 0 or enlarges to 1, we say that they become synchronized. In the following,  $\phi_k$  is the phase of oscillator  $k$  when it reacts,  $\Delta\phi_k$  is the phase jump amount of oscillator  $k$  after its reaction. First, when oscillator  $B$  is fired,  $A$  jumps (Figure 2(b,c)),  $AB$  distance changes to

$$|\overrightarrow{A'B'}| = |\overrightarrow{AB}| - \Delta\phi_A \quad (1)$$

Then, both oscillators move forward until  $A$  fires. After  $B$  jumps (Figure 2(d, e)), the distance becomes:

$$|\overrightarrow{A''B''}| = |\overrightarrow{A'B'}| + \Delta\phi_{B'} = |\overrightarrow{AB}| - \Delta\phi_A + \Delta\phi_{B'} \quad (2)$$

$$|\overrightarrow{AB}| - |\overrightarrow{A''B''}| = \Delta\phi_A - \Delta\phi_{B'} \quad (3)$$

To compare the value of  $|\overrightarrow{A''B''}|$  and  $|\overrightarrow{AB}|$ , the relationship of  $\Delta\phi_A$  and  $\Delta\phi_{B'}$  is needed. To get that, the monotonicity of  $\Delta\phi_k$  and the two oscillators' jump position  $\phi_A$  and  $\phi_{B'}$  are checked:

**Step 1.** To judge the monotonicity of  $\Delta\phi_k$  we calculate its derivative:

$$\Delta\phi_k = f^{-1}(f(\phi_k) + \epsilon) - f^{-1}(f(\phi_k)) \quad (4)$$

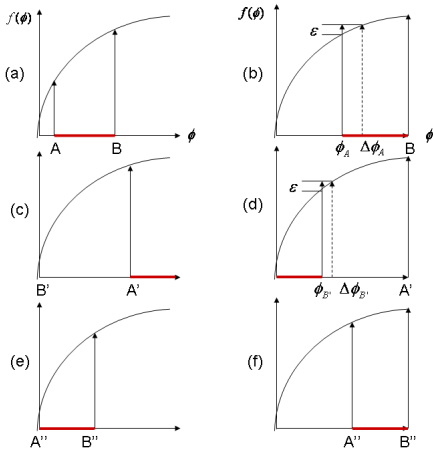


**Figure 2. A pair nodes phase converging procedure in one cycle.**

$$\begin{aligned} \Delta\phi'_k &= \frac{1}{f'(f^{-1}(f(\phi_k) + \epsilon))} - \frac{1}{f'(f^{-1}(f(\phi_k)))} \\ &= \frac{f'(f^{-1}(f(\phi_k))) - f'(f^{-1}(f(\phi_k) + \epsilon))}{f'(f^{-1}(f(\phi_k) + \epsilon))f'(f^{-1}(f(\phi_k)))} \end{aligned} \quad (5)$$

For  $f' > 0$ ,  $f$  and  $f^{-1}$  both are monotonically increasing. And  $f'' < 0$ , so  $f'(f^{-1}(f(\phi_k))) > f'(f^{-1}(f(\phi_k) + \epsilon))$ ,  $\Delta\phi'_k > 0$ .  $\Delta\phi_k$  is monotonically increasing follow the increasing of phase  $\phi_k$ . The coupling happened in later position always causes bigger phase jump amount than its former ones.

**Step 2.** Consider the two oscillators' jumping position  $\phi_A$  and  $\phi_{B'}$  (Figure 2(b, c, d)). When  $\phi_B$  is at critical firing point ( $\phi_B = 1$ ):

$$\phi_{B'} = 1 - \phi_{A'} = 1 - f^{-1}(f(\phi_A) + \epsilon) \quad (6)$$

$$\phi_A - \phi_{B'} = \phi_A + f^{-1}(f(\phi_A) + \epsilon) - 1 \quad (7)$$

**Step 3.** Combine equation (7) with equation (3):

When  $\phi_A + f^{-1}(f(\phi_A) + \epsilon) > 1$ ,  $\phi_A > \phi_{B'}$ ; for monotonically increasing of  $\Delta\phi_k$ ,  $\Delta\phi_A > \Delta\phi_{B'}$ , so  $|\overrightarrow{A''B''}| < |\overrightarrow{AB}|$ . In next cycle, when  $\phi_{B''} = 1$ , for  $|\overrightarrow{A''B''}| < |\overrightarrow{AB}|$ ,  $A$ 's new phase  $\phi_{A''}$  must be bigger than  $\phi_A$ , so in the afterwards, it will always meet the requirement  $\phi_A + f^{-1}(f(\phi_A) + \epsilon) > 1$ ;  $|\overrightarrow{AB}|$  value will continue shrinking until equal to 0.

When  $\phi_A + f^{-1}(f(\phi_A) + \epsilon) < 1$ ,  $\phi_A < \phi_{B'}$ ,  $\Delta\phi_A < \Delta\phi_{B'}$ , then  $|\overrightarrow{A''B''}| > |\overrightarrow{AB}|$ . For the same reason, the new phase of  $A$  will always drop in this case,  $|\overrightarrow{AB}|$  will continue enlarging until equal to 1.

When  $\phi_A + f^{-1}(f(\phi_A) + \epsilon) = 1$ ,  $\phi_A = \phi_{B'}$ ,  $\Delta\phi_A = \Delta\phi_{B'}$ , then  $|\overrightarrow{A''B''}| = |\overrightarrow{AB}|$ . This is the unique fixed point. Actually, for the uniqueness of this point and clock drift or

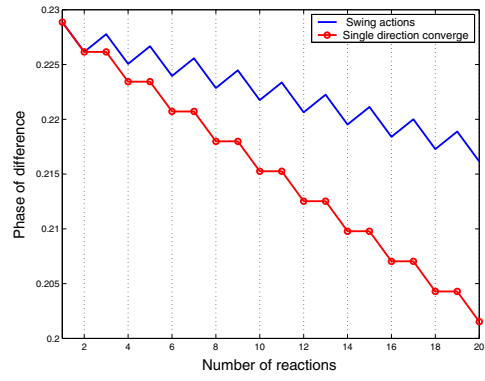


**Figure 3. Swing action of the phase difference.**

clock measurement errors, once the phase drifts away a little, the system will push the phase to the 1 or 0 synchronicity state. So the existence of an unique fixed point will not cause a system pause but it is a 'repeller' as described in [7].

Following from the above steps, the pair oscillators' Converging Direction Determinant Formula is determined:

**Lemma 1** Given pair oscillators, with one at the edge of firing, one at phase  $\phi_k$ . Define  $D_k$  is the phase difference between them. Follow the pulse coupling dynamics,  $\phi_{k,J} = f^{-1}(f(\phi_k) + \epsilon)$  is the phase after reacting the incoming pulse.

If  $V_k = \phi_k + \phi_{k,J} > 1$ , then after one cycle, the two oscillators converge and finally  $D_k$  will converge to 0;

if  $V_k = \phi_k + \phi_{k,J} < 1$ , then after one cycle, the two oscillator diverge and finally  $D_k$  will converge to 1.

From the format of the determinant formula, observe that the pair initial phase states, the coupling strength  $\epsilon$  and the extent to which  $f(\phi)$  is concave down all influence the converging procedure.

## 4 Selective pulse coupling algorithm

### 4.1 Single Direction Converge

As we observed, for each oscillator pair, when one fires, if they are not converged then their converging direction will change. The phase difference swings:  $|\overrightarrow{AB}| > |\overrightarrow{A'B'}|$  and  $|\overrightarrow{A'B'}| < |\overrightarrow{A''B''}|$ . The distance is decreased then increased in a single cycle. Except the last jump before final synchronizing, every jump does not cause the phase distance change by  $\Delta\phi$  but by  $\Delta(\Delta\phi)$ . Figure 3 illustrates the phase difference swing actions of a pair of oscillators (the upper line). The swing between two directions prolong the converging time and consume more energy.

The swing actions are actually the phase difference attempting to search the final converging direction: does the

difference enlarge to 1 or shrink to 0? So if the converging direction is known in advance, then the reverse direction jump become unnecessary. Specifically, when an oscillator detects one pulse, it calculates its  $V_k$  value and checks that the coming jump is to its final converging direction, or not. If it is, then react to the firing pulse, jump the oscillator phase; otherwise, ignore the pulse, do nothing. Thus, the reverse direction jumping is replaced by just keeping its original place, and the up-jump segments in the upper line become the level segments in the lower line as shown in Figure 3.

## 4.2 Multi-nodes Multi-hop situation

For a multi-hop situation, every firing pulse can only affect the oscillators in its neighboring area for local coupling. The converging starts from one or several points then gradually spreads to the whole network. For the asynchronous coupling, the phase order may change after each firing. In the present firing cycle, the oscillator which has its phase nearing to the firing threshold becomes the next firing oscillator. The system is totally dynamic and self-organizing.

On the other hand, in multi-nodes networks, one oscillator will receive more than one firing pulse per cycle. The total jump amount in one direction relates to the number of coupling and the coupling happened position before itself firing. However, these two things change at each cycle for the dynamic nodes firing order. It is not easy to tell the node's final converging direction in the beginning of converging procedure. So only the current oscillator phase distribution information can be used. Using the local optimization principle, we propose: *Each node, once 'hearing' the pulse, judges if the phase distance between itself and the firing one will converge or diverge, then decides to react to the firing node or not.* Each oscillator chooses the firing one that has the same converging direction with itself at this time to react. Although this can not eliminate all the swings, it can avoid the obvious reverse direction jumps so as quicken the total converging progress. We call it as our Selective Coupling Synchronicity Algorithm (SCSA).

In the Selective Coupling Synchronization Algorithm, nodes transmit simple pulses instead of packet messages as the time signal. And although receivers selectively react to the incoming pulse, they still do not need to identify the source of emission and require no memory to store time information of other nodes. So this algorithm can be operated at physical layer or implemented on hardware totally. Therefore, the imprecision due to MAC layer delays, protocol processing or software implementation does not exist. Also from a physical layer perspective, a synchronization process where all nodes transmit the same word is not affected by collisions in a similar way to flooding [9]. To maintain the system stability [10], We also assign a refrac-

tory period right after nodes' own firing, during which no signal can be received from other nodes.

---

### Algorithm 1 Selective Pulse Coupling synchronicity

---

```

1. while (not synchronized) do
2.   Advance all phases until the highest one fires
3.   for (every firing pulse) do
4.     for (every non-firing receiver) do
5.       if (not jumped yet) and (within transmission
           range) then
6.         Calculate  $\phi_{k,J} = f^{-1}(f(\phi_k) + \epsilon)$ 
7.         if  $V_k = \phi_k + \phi_{k,J} > 1$  then
8.           React to the pulse and mark as jumped
9.         else
10.          Ignore this pulse
11.        end if
12.      end if
13.    end for
14.  end for
15. end while

```

---

The pseudo-code describes the operations happened during the whole synchronizing procedure. Every node periodically follows its oscillating trajectory. Only when detecting a firing pulse, the node calculates the post jumping phase value  $\phi_{k,J} = f^{-1}(f(\phi_k) + \epsilon)$ , judges its next converging direction and decides to react to the pulse or not. Here, judging and calculating do not bring much additional overhead to the system, because even without the converging direction checking, it also needs to calculate the post jumping phase value  $\phi_{k,J}$  for reacting to the pulse. Our Selective Coupling Algorithm only brings one more addition and one additional comparison operation with every firing.

## 5 Performance evaluation

### 5.1 Evaluation Metrics

Our algorithm aims to increase the converging efficiency, so we mainly evaluate the converging speed and the associated energy consumption of selective coupling synchronicity algorithm compared with the all pulse coupling model.

**Time to Sync:** The amount of time until the system achieves synchronicity. We use the number of the oscillator's natural period  $T_o$  to measure the converging time.

**Energy to Sync:** For sensor nodes, energy consumed by communication is much greater than that by calculation or sensing. We count the total number of pulse emitted by the entire network of nodes before synchronicity is achieved. Multiplying this number by  $r^2$ , the square of the transmission radius. we obtain the total energy

consumption normalized by the energy of a single pulse necessary to reach a transmission range equal to 1 [3].

## 5.2 Simulation Results

In the simulation, oscillator hardware constraints are considered: oscillator is not allowed to jump or fire continuously for the refractory period; and oscillators do not detect the strength of pulses for simplicity. Clock skew that occur from variations in clock crystals in individual wireless sensors are not considered.

We choose  $f(\phi) = \frac{1}{b} \ln[(e^b - 1)\phi + 1]$  as the oscillator function in our simulation (similar to the function selected in [7]). For the coupling strength  $\epsilon$  and the extent of function  $b$  have similar effect on the rate of synchrony, set  $b = 1$  therefore  $f(\phi) = \ln[(e - 1)\phi + 1]$ . Refer to [9], refractory period is set  $T_{refr} = 0.01T_o$ . We also set the maximum acceptable converging time as  $2000T_o$ , if within this period the network does not synchronized, we regard the converging procedure failed.

$N$  nodes are distributed randomly within a  $10 \times 10 m^2$  network area with connectivity. In random topology, nodes locally communicate with other nodes within the transmission range  $r$ . When  $r$  near or greater than  $10\sqrt{2}$  it becomes all-to-all coupling. All initial phase states are randomly distributed with uniform distribution. And all the results are averaged over 500 network topologies and initial phases realization.

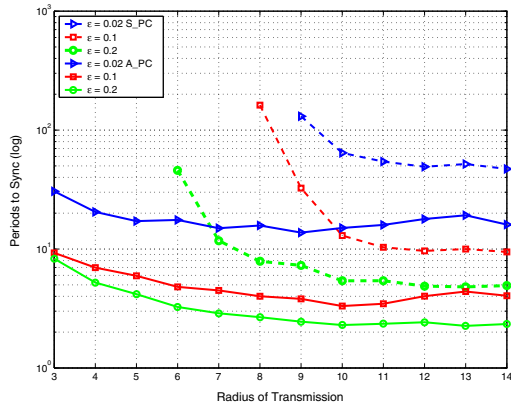


**Figure 4. A\_PC/S\_PC Average locking time versus the transmission range with  $\epsilon = 0.02, 0.1, 0.2$ , and  $1nodes/m^2$ .**

Figure 4 shows the comparison of converging time between our selective pulse coupling algorithm(S\_PC) and all pulse coupling model(A\_PC) under the different parameter settings. First, as proved in [7], proper stronger coupling strength  $\epsilon$  causes higher synchronizing rate. This also works for selective coupling situation. Second, when transmission radius  $r$  is not big enough ( $r < 3$  for S\_PC and

$r < 6$  for A\_PC), the converging speed is too slow to accept for sparsity of coupling nodes. As  $r$  increases, converging speed increases also; when nodes near to all-to-all coupling ( $r \geq 11$ ), the converging speeds reach maximum and remain similar later. Here we can see all pulse coupling model brings a high demand on the node deployment and initial phases. While our algorithm can guarantee convergence under poor coupling situation, because the selective coupling enable fast converge in the correct direction and restrain the reverse direction attempts. Fasting the firing step in local area will bring ripple effect to the whole network so as the network's converging time also hasten greatly. Above all, under the same parameter settings, our selective coupling algorithm always have high synchronizing speed than all pulse coupling model.

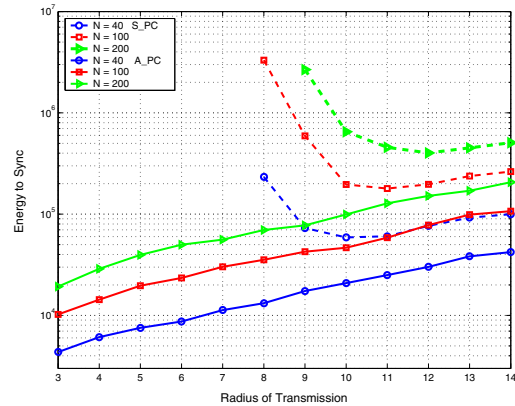


**Figure 5. A\_PC/S\_PC Average total energy consumption of the entire network versus the transmission range with  $0.4nodes/m^2$ ,  $1nodes/m^2$ ,  $2nodes/m^2$ , when  $\epsilon = 0.1$ .**

From figure 5 we got some observations. All pulse coupling model has a local minimum point for energy consumption with some transmission radius. Because although smaller transmission radius needs less transmission power which is directly proportional to square of the transmission radius, it also may need more pulses transmitted to get converge. There is a tradeoff between transmission power for each pulse and the number of pulse. While for selective coupling algorithm, the increased transmission radius has more weight than the decreased converging time. For our algorithm, the smallest radius brings lowest energy consumption. We also observe that the more nodes in network, the more energy needed to reach synchronization, but for each node, the energy consumed does not have much difference. Under the same condition, to reach synchronization, our selective coupling algorithm consume less energy.

Combine the discussions of figure 4 and 5, figure 6 gives out the relationship between synchronizing time and the associated energy consumption of selective coupling synchrono-

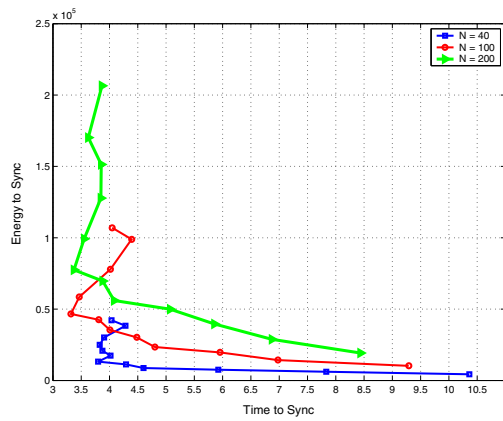


**Figure 6. S\_PC Average total energy consumption of the entire network to reach synchronization versus the time need to synchronization when  $\epsilon = 0.1$ .**

nization algorithm. In the figure, the lower left corner represents the ideal situation for all algorithms, which has the highest converging speed while consumes the least energy, on the contrary, the upper right corner represents the worst case. So for every line, the point who is nearest to the bottom left point has the optimal efficiency. With the help of these lines, we can choose the proper transmission radius according the different application requirements or limitations.

## 6 Conclusion

Mutual synchronization inspired from biological system represents the new trend in time synchronization in sensor networks. It is simple, robust, self-organizing and easy to implemented on hardware. Based on the pulse coupling biological oscillator model our proposed Selective Coupling Synchronicity Algorithm (SCSA) addresses the problem of low efficiency caused by the phase swing actions in the original pulse coupling model. It gains the fast synchronizing speed and lower associated energy consumption. As the theoretical basement, the Converging Direction Determinant Formula also has been derived.

For the future work, the effect caused by the variations of the intrinsic oscillator frequency and the relationship between synchronicity precision and the refractory period length will be investigated.

## Acknowledgment

This research was supported by the MKE (Ministry of Knowledge Economy), Korea, under the ITRC (Information Technology Research Center) support program supervised by the IITA (Institute of Information Technology Advancement) (IITA-2008-C1090-0801-0002) and by the MIC (Ministry of Information and Communication), Korea,

Under the ITFSIP (IT Foreign Specialist Inviting Program) supervised by the IITA (Institute of Information Technology Advancement, C1012-0801-0003).

Also, this work is financially supported by the Ministry of Education and Human Resources Development (MOE), the Ministry of Commerce, Industry and Energy (MOCIE) and the Ministry of Labor (MOLAB) through the fostering project of the Lab of Excellency.

## References

- [1] J. Elson, L. Girod, and D. Estrin. Fine-grained network time synchronization using reference broadcasts. In *Fifth Symposium on Operating Systems Design and Implementation (OSDI 2002)*, pages 147–163, Boston, Massachusetts, USA, Dec 2002. USENIX Association.
- [2] S. Ganeriwal, R. Kumar, and M. Srivastava. Timing-sync protocol for sensor networks. In *Proc. 1st ACM Conference on Embedded Networked Sensor Systems (SenSys'03)*, pages 138–149, Los Angeles, California, USA, Nov 2003. ACM Press.
- [3] S. A. Hong Yao-Win. A scalable synchronization protocol for large scale sensor networks and its applications. *IEEE Journal on Selected Areas in Communications*, 23(5):1085–1099, May 2005.
- [4] J. Sallai, B. Kusy, A. Prabal, and P. Dutta. On the scalability of routing-integrated time synchronization. In *Proc. 3rd European Workshop on Wireless Sensor Networks (EWSN)*, pages 115–131, Zurich Switzerland, Feb 2006.
- [5] B. Kusy and M. Maroti. Flooding time synchronization in wireless sensor networks. In *Proc. 2nd ACM Conference on Embedded Networked Sensor Systems (SenSys'04)*, pages 39–49, Baltimore, Maryland, USA, Nov 2004. ACM Press.
- [6] D. Lucarelli and I. Wang. Decentralized synchronization protocols with nearest neighbor communication. In *Proc. 2nd ACM Conference on Embedded Networked Sensor Systems (SenSys'04)*, pages 62–68, Baltimore, Maryland, USA, Nov 2004.
- [7] R. Mirollo and S. Strogatz. Synchronization of pulse-coupled biological oscillators. *SIAM Journal on Applied Mathematics*, 50(6):1645–1662, Dec 1990.
- [8] K. Romer. Time synchronization in ad hoc networks. In *Proc. of the 2nd ACM Int'l Symp. on Mobile Ad Hoc Networking and Computing (MOBIHOC 01)*, pages 173–182, Long Beach, CA, USA, Oct 2001. ACM Press.
- [9] A. Tyrrell, G. Auer, and C. Bettstetter. Fireflies as role models for synchronization in ad hoc networks. In *Proc. Intern. Conf. on Bio-Inspired Models of Network, Information, and Computing Systems (BIONETICS)*, Dec 2006.
- [10] K. P. U. Ernst and T. Geisel. Synchronization induced by temporal delays in pulse-coupled oscillators. *Physical Review Lett*, 74(19):1570C1573, Feb 1995.
- [11] G. Werner-Allen, G. Tewari, A. Patel, M. Welsh, and R. Nagpal. Firefly inspired sensor network synchronicity with realistic radio effects. In *Proc. 3rd ACM Conference on Embedded Networked Sensor Systems (SenSys'05)*, pages 142–153, San Diego, California, USA., November 2005. ACM Press.